

Numerical Simulation of the Turbulent Two-Phase Jet

IVAN V. KAZACHKOV

Department of Information Technology and Data Analysis
Nizhyn Mykola Gogol State University

16600 Graftska str. 2, Nizhyn

UKRAINE

kazachkov.iv@ndu.edu.ua, ivan.kazachkov@energy.kth.se

Abstract: - The paper is devoted to the mixing and heat transfer features of mutually immiscible liquids in the two-fluid turbulent heterogeneous jet flow. Differential equations for the axially symmetrical two-dimensional stationary flow were solved numerically. Parameters of the turbulent mixing were simulated and analyzed. The phenomenon of amplification of a jet's kinetic energy against the input energy of the first phase at the nozzle was revealed in numerical simulation and discussed. The experimental data with water and oil, as well as with liquid metals, confirmed the results of numerical computer simulation. The method may be applicable for the tasks, where the parameters of multiphase turbulent mixing and heat transfer are important.

Key-Words: - Two-Phase Turbulent Jet; Mutually Immiscible Liquids; Function-Indicator; Numerical Simulation; Experimental Study

I. STATEMENT OF THE PROBLEM

This paper is prolongation of the first paper on the subject presented together with this one in this journal [1]. Therefore, we do not repeat the basics by methods applied, except the general statement. And detail analysis of the literature sources has been done in [1], so that let us just mention here additionally that some relevant studies can be also found in [2, 3].

A. Mathematical Model for Turbulent Two-Phase Jet of Mutually Immiscible Liquids

The method for modeling the turbulent heterogeneous jets of the mutually immiscible liquids was proposed by Prof. Nakorchevskii [4].

According to it all parameters $a^l(t)$ (density of liquid, flow velocity, temperature, etc.) of a

multiphase mixture with the phase interfaces, like oil and water mixture, are considered as follows:

$$a^l(t) = \sum_{i=1}^m B_i(t) a_i^l(t), \quad \sum_{i=1}^m B_i = 1.$$

The function-indicator $B_i(t)$ is introduced for the phases in multiphase flow by the next rule:

$$B_i(t) = \begin{cases} 1, & i\text{-phase occupies elementary volume } \delta V \\ 0, & i\text{-phase outside elementary volume } \delta V \end{cases}$$

It shows the content of each phase in each elementary volume of the flow.

The method was successfully applied for solution of the multiple problems [5-8]. This paper continues [1], where the mathematical models for the initial and ground parts of the turbulent two-phase jet have been developed and analyzed in detail.

B. Boundary Problem for Initial Part of Jet

Differential equation array for the radius of the potential core $y_0(\zeta)$ and the function $h(\zeta)$ is the following [1]:

$$\frac{dh}{d\zeta} = -\frac{1}{y_0^3 D_2} \cdot \frac{dy_0}{d\zeta}, \quad (1)$$

$$\frac{dy_0}{d\zeta} = y_0^2 D_2 \left(1 + A\eta^*\right) \frac{B_1^* \left(\frac{\partial u_1}{\partial \eta}\right)^* + i_0 \kappa_{21} B_2^* \left(\frac{\partial u_2}{\partial \eta}\right)^*}{(1 - u_1^* + 2D_1) y_0^2 D_2 - \frac{dD_1}{dh}}.$$

Here the function $h(\zeta)$ describes variation of the function-indicator $B_i(t)$ against axis of a jet [1]. The next parameters are taken according to [4]:

$$(\partial u_2 / \partial \eta)^* = (\partial u_1 / \partial \eta)^* = -1.5, \quad B_1^* = B_1(\eta^*),$$

$$\partial u_1 / \partial \eta = 12\eta^2(\eta - 1), \quad \partial u_2 / \partial \eta = -12\eta(\eta - 1)^2,$$

$$u_1^* = 11/16, \quad u_2^* = 5/16, \quad A = \frac{a_3 + i_0 b_3 - a_1}{a_2 - i_0 b_4 - a_4},$$

$$D_1 = A \left[a_3^* + i_0 b_3^* - a_1^* u_1^* - i_0 b_1^* u_2^* + \right. \\ \left. + A \left(a_4^* + i_0 b_4^* - a_2^* u_1^* - i_0 b_2^* u_2^* \right) \right],$$

$$\frac{dA}{dh} = \frac{a_{32} + i_0 b_{32} - a_{12}}{a_2 - i_0 b_4 - a_4} - A \frac{a_{22} - i_0 b_{42} - a_{42}}{a_2 - i_0 b_4 - a_4},$$

$$D_2 = a_{22} A^2 + A \left(a_{12} + 2a_2 \frac{dA}{dh} \right) + a_1 \frac{dA}{dh},$$

$$\frac{dD_1}{dh} = \frac{dA}{dh} \left(a_3^* + i_0 b_3^* - a_1^* u_1^* - i_0 b_1^* u_2^* \right) + \\ A \left(a_{32}^* + i_0 b_{32}^* - a_{12}^* u_1^* - i_0 b_{12}^* u_2^* \right) + \\ + 2A \frac{dA}{dh} \left(a_4^* + i_0 b_4^* - a_2^* u_1^* - i_0 b_2^* u_2^* \right) + \\ A^2 \left(a_{42}^* + i_0 b_{42}^* - a_{22}^* u_1^* - i_0 b_{22}^* u_2^* \right).$$

And the radius of potential core is connected with the radius of mixing zone as follows [1, 4]:

$$y_0 = \frac{1}{\sqrt{1 + 2a_1 \frac{a_3 + i_0 b_3 - a_1}{a_2 - i_0 b_4 - a_4} + 2a_2 \left(\frac{a_3 + i_0 b_3 - a_1}{a_2 - i_0 b_4 - a_4} \right)^2}},$$

$$\delta = y_0 \frac{a_3 + i_0 b_3 - a_1}{a_2 - i_0 b_4 - a_4}. \quad (2)$$

The boundary conditions are:

$$\zeta=0, \quad y_0=1, \quad \delta=0, \quad h=h_0=h(0); \quad (3)$$

$$\zeta=\zeta_i, \quad y_0=0, \quad \delta=\delta_i, \quad h=h_i=h(\zeta_i), \quad (4)$$

$$h_0 = \frac{a_{11} - a_{31} - i_0 b_{31}}{a_{32} - a_{12} + i_0 b_{32}}, \quad h_i = \frac{a_{21} - a_{41} - i_0 b_{41}}{a_{42} - a_{22} + i_0 b_{42}}.$$

The boundary conditions (3) are used in numerical solution of the equation array (1), (2), while the conditions (4) determine the boundaries of the jet and the limit values of the parameters. $h(x) = \partial^2 B_1 / \partial \eta^2$.

1.3 Boundary Problem for the Ground Part

For the ground part of a jet the following equation array and the boundary conditions are solved [1, 4]:

$$h = \frac{\alpha_{11} - (\alpha_{21} + i_0 \beta_{21}) u_{m1} - 2i_0 \alpha_{11} \beta_{20} u_{m1}^2 \delta^2}{-\alpha_{12} + (\alpha_{22} + i_0 \beta_{21}) u_{m1} + 2i_0 \alpha_{12} \beta_{20} u_{m1}^2 \delta^2},$$

$$B_{m1} = \frac{2i_0}{Z} \alpha_{12} \beta_{20} + \frac{\alpha_{22} + i_0 \beta_{22}}{Z u_{m1} \delta^2} - \frac{\alpha_{12}}{Z u_{m1}^2 \delta^2}; \quad (5)$$

$$\frac{du_{m1}}{d\zeta} = 2 \frac{u_{m1}}{\delta} \frac{(u_1^*)_0 B_{m1} + i_0 \kappa_{21} (1 - B_{m1}) (u_2^*)_0}{B_{m1} + i_0 (1 - B_{m1})}, \quad (6)$$

$$\frac{d\delta}{d\zeta} = \frac{1}{D_1 u_{m1}^2 \delta} \left[\left(M_1 + u_{m1} \delta^2 M_2 + \frac{M_3}{u_{m1}} \right) f_1 + \right. \\ \left. + 0.75 \left(\frac{N_3}{\delta} + \frac{N_2 u_{m1}}{\delta} + N_1 u_{m1}^2 \delta \right) \right];$$

$$\zeta = 0, \quad u_{m1} = 1, \quad \delta = \delta_i. \quad (7)$$

Here are:

$$M_2 = \frac{2i_0}{Z} \beta_{20} \left\{ 2 \left[\alpha_{12} (\alpha_{21}^* + i_0 \beta_{21}^*) - (\alpha_{22}^* + i_0 \beta_{22}^*) \alpha_{11} \right] + \left[\alpha_{11} (\alpha_{12}^* u_1^* + \right. \right. \\ \left. \left. + i_0 \beta_{12}^* u_2^*) - \alpha_{12} (\alpha_{11}^* u_1^* + i_0 \beta_{11}^* u_2^*) \right] \right\} + \\ + i_0 (2\beta_{20}^* - \beta_{10}^* u_2^*), \quad f = \frac{du_{m1}}{d\zeta},$$

$$M_1 = \frac{1}{Z} \left[(\alpha_{21}^* + i_0 \beta_{21}^*) (\alpha_{22} + i_0 \beta_{22}) + \right. \\ \left. - (\alpha_{22}^* + i_0 \beta_{22}^*) (\alpha_{21} + i_0 \beta_{21}) \right],$$

$$M_3 = \frac{\alpha_{11} (\alpha_{12}^* u_1^* + i_0 \beta_{12}^* u_2^*) - \alpha_{12} (\alpha_{11}^* u_1^* + i_0 \beta_{11}^* u_2^*)}{Z},$$

$$N_3 = \frac{1}{Z} (\alpha_{12} \gamma_1 - \alpha_{11} \gamma_2) (i_0 \kappa_{21} - 1),$$

$$D_1 = \frac{4i_0}{Z} \beta_{20} \left[\alpha_{11} (\alpha_{22}^* + i_0 \beta_{22}^*) - \alpha_{12} (\alpha_{21}^* + i_0 \beta_{21}^*) + \right. \\ \left. + \alpha_{12} (\alpha_{11}^* u_1^* + i_0 \beta_{11}^* u_2^*) - \alpha_{11} (\alpha_{12}^* u_1^* + i_0 \beta_{12}^* u_2^*) \right] + \\ + 2i_0 (\beta_{10}^* u_2^* - \beta_{20}^*), \quad N_1 = \frac{2i_0}{Z} \beta_{20} i_0 \kappa_{21}.$$

$$\cdot (\alpha_{12} \gamma_1 - \alpha_{11} \gamma_2) \left[1 - \frac{2i_0}{Z} \beta_{20} (\alpha_{12} \gamma_1 - \alpha_{11} \gamma_2) \right],$$

$$N_2 = \frac{1}{Z} \left\{ i_0 \kappa_{21} \left[\gamma_2 (\alpha_{12} + i_0 \beta_{21}) - \gamma_1 (\alpha_{22} + i_0 \beta_{22}) \right] + \right. \\ \left. + \gamma_1 (\alpha_{22} + i_0 \beta_{22}) - \gamma_2 (\alpha_{21} + i_0 \beta_{21}) \right\}.$$

The boundary problem (6), (7) was solved numerically with a control of the value h and automatic transforming of the approximation B_1 according to the determined ranges of each of them [1]. The functions $u_{m1}(\zeta)$, $B_{m1}(\zeta)$, $\delta(\zeta)=0$, and $h(\zeta)$ were computed for a range of parameters i_0, κ_{21} .

The control parameters were chosen according to (5) under requirements: $B_{m1} < 1$, $u_{m1} < 1$, $dB_{m1}/d\zeta < 0$, $d\delta/d\zeta > 0$. The first one means that after the initial part of the jet, when potential core is spent, the

content of the first phase in a mixture of phases will gradually fall down due to increase of the ejected phase. The velocity of a flow (including on the axis) is decreasing with loose of energy and expanding of the mixing layer due to this.

Analysis of the performed numerical simulations showed that solution of the equation (7) is correct only for the restricted ratio of the turbulent mixing coefficients κ_{21} specific for each value of i_0 . It's an interesting feature that a ratio of the turbulent mixing coefficients of the phases cannot be arbitrary, which seems to be physically reasonable.

For an average value κ_{21}^{av} and for variation range $\Delta\kappa_{21}$, the following approximations were obtained: $\kappa_{21}^{av} = 0.2 / i_0$, $\Delta\kappa_{21} = \pm 0.02i_0$. The higher is density of the ejected liquid, the lower is its mixing coefficient comparing to a first liquid. But possible interval of the ratio can grow with i_0 .

1.4 Parameters of the Ground Part of a Jet

The parameters of the ground part of a jet are as follows: $\beta_{10}=0.1$, $\beta_{20}=11/210$, $\beta_{10}^*=0.07344$, $\beta_{20}^*=0.04777$. Another parameters, $\alpha_{ij}, \beta_{ij}, \alpha_{ij}^*, \beta_{ij}^*$ are given in the Tables 1, 2:

Table 1 – Integral parameters $\alpha_{ij}, \alpha_{ij}^*$ for different regions of the function-indicator B_1

α_{ij} for h :	α_{11}	α_{12}	α_{21}	α_{22}
$h \in [0, -6]$	9/70	7.143e-3	61/770	3.301e-3
$[-6, -12]$	89/840	3.373e-3	65/924	1.822e-3
$[-12, -20]$	73/840	1.786e-3	527/8580	1.078e-3
$[-20, -30]$	221/3080	1.028e-3	267/5005	6.743e-4
α_{ji}^* for h :	α_{11}^*	α_{12}^*	α_{21}^*	α_{22}^*
$h \in [0, -6]$	0.086747	3.083e-3	0.065782	2.090e-3
$[-6, -12]$	0.079832	1.931e-3	0.06130	1.342e-3
$[-12, -20]$	0.07148	1.235e-3	0.05576	8.81e-4
$[-20, -30]$	0.06293	8.070e-4	0.04996	5.909e-4

Table 2 – Integral parameters β_{ij}, β_{ij}^* for different regions of the function-indicator B_1

β_{ij} for h :	$-\beta_{11}$	$-\beta_{12}$	$-\beta_{21}$	$-\beta_{22}$
$h \in [0, -6]$	19/210	4.1(6)e-3	43/858	1.573e-3

$[-6, -12]$	11/140	2.183e-3	698/15015	9.685e-4
$[-12, -20]$	311/4620	1.245e-3	212/5005	6.244e-4
$[-20, -30]$	19/330	0.(75)e-3	1531/4004 0	4.183e-4
β_{ji}^* for h :	$-\beta_{11}^*$	$-\beta_{12}^*$	$-\beta_{21}^*$	$-\beta_{22}^*$
$h \in [0, -6]$	0.070629	2.328e-3	0.046421	1.257e-3
$[-6, -12]$	0.065555	1.482e-3	0.04389	8.349e-4
$[-12, -20]$	0.05934	9.64 e-4	0.04067	5.668e-4
$[-20, -30]$	0.05288	6.412e-4	0.03720	3.931e-4

Thus, with the above stated boundary problem and the calculated integral parameters presented in the tables 1, 2 the mathematical model for the heterogeneous turbulent jet is complete.

An interesting feature was revealed for the influence of parameters i_0, κ_{21} on the solution. The radius of a jet and velocities of phases on axis practically don't depend on κ_{21} being totally determined by the value i_0 , while the functions B_{ml} and h strictly depend on κ_{21} . Thus, the turbulent mixing mostly influences the internal structure of a flow, distribution of the phases, while velocities depend on the density ratio of the phases (internal structure has little influence on it). The velocity distribution, in a turn, determines a radius of mixing zone because it changes with falling of the velocity according to the mass and momentum equations.

Due to absence of the proven methodology for calculation of the transient part, the ground part of a jet was proposed for investigation in the following way, independent of the limitations by κ_{21} . As far as two functions, B_{ml} and h , determine the function B_1 , and influence of B_{ml} is stronger than h , one can assume $h=h_t=const$ for the ground part, so that B_{ml} is correcting a possible inaccuracy. This assumption is overdetermined; therefore, a radius of the mixing zone δ is calculated by two different ways independently. Controlling the ratio of δ_1 and δ_2 computed from two different equations allowed decide upon attainability of this assumption, as well as upon a total inaccuracy of the model.

The equations (5) yield:

$$B_{m1} = \frac{\beta_{20}i_0}{\frac{\alpha_{11} + \alpha_{12}h_t}{u_{m1}} - \alpha_{21} - i_0\beta_{21} - (\alpha_{22} + i_0\beta_{22})h_t},$$

$$\delta = \frac{1}{\sqrt{2B_{m1}u_{m1}(\alpha_{11} + \alpha_{12}h_t)}}. \quad (8)$$

The first correlation (8) shows dependence of the function-indicator of the first phase on the axis of a jet against velocity of the first phase on the axis and integral parameters of a flow. The second correlation (8) describes variation of the radius of mixing layer depending on the axial velocity and function-indicator (content of the first phase on the axis of a flow).

II. SIMULATION OF TWO-PHASE JET FLOW

2.1 Calculation of Jet Flow at the Initial Part

The boundary problem (1)-(4) can be solved numerically directly but we have investigated more simple and accurate solution procedure described here. After substitution of the computed functions $y_0(h)$ $\delta(h)$, the equation array (1)-(4) was solved as follows. Velocity distributions for the phases (u_1, u_2) and function-indicators of the phases (B_1, B_2) were stated together with the values of parameters at the cross section of the nozzle.

The system (1), (2) contains two algebraic and differential equations. The functions $y_0(h)$, $\delta(h)$ were got from the algebraic equation array. Then differential equation was expressed in the following standard form

$$dh/d\zeta = F(h(\zeta), i_0, \kappa_{21}). \quad (9)$$

Function $FM=1/F$ was computed in the range of parameters: $i_0=[0.2;16]$, $\kappa_{21}=[0;5]$, $h=[-20;0]$. Its approximation was found as $FM=A_1' + A_2'h + A_3'h^2$, where $A_i'(i_0, \kappa_{21})$ - functions computed with the accuracy over 0.2%.

Solution of the equation (9) with an account of the above-mentioned results in

$$\zeta = A_0 + A_1h + A_2h^2 + A_3h^3, \quad (10)$$

where $A_0 = -A_1h_0 - A_2h_0^2 - A_3h_0^3$, $A_i = A_i'/i$, $i=1,2,3$. The functions $A_i(i_0, \kappa_{21})$, $\zeta_i(i_0, \kappa_{21})$, $i=1,2,3$, for 3 different values of the parameter i_0 are presented in Fig 1. Thus, $\zeta_i = A_0 + A_1h_i + A_2h_i^2 + A_3h_i^3$. The maximal total inaccuracy of computation after integration of (9) estimated by the Cauchy-Bunyakovsky inequality satisfied the condition $D_{\max} < D_{\max}(Dh)_{\max}$. The estimation showed $(Dh)_{\max} < 4$, and $D_{\max} < 0.8\%$, which is attainable for the integral methods in turbulent jets [8-11].

Solution of the boundary problem (1)-(4) allows obtaining the parameters for the initial part of a jet by the stated values i_0, κ_{21} . The correlations (2) allows computing $y_0(h)$, $\delta(h)$ and current radius of a jet $r = y_0(h) + \delta(h)$, as well as the function-indicator of

phases shown in Figs 2, 3 (1- $\kappa_{21}=0.2$, 2- $\kappa_{21}=1$, 3- $\kappa_{21}=5.0$).

Computation showed that the length of the initial part of a jet strictly depends on a ratio of the turbulent mixing coefficients: the higher is turbulent mixing in a second phase, the longer is an initial part. Strong mixing in a first phase means physically that it keeps parameters of the first phase for a long time.

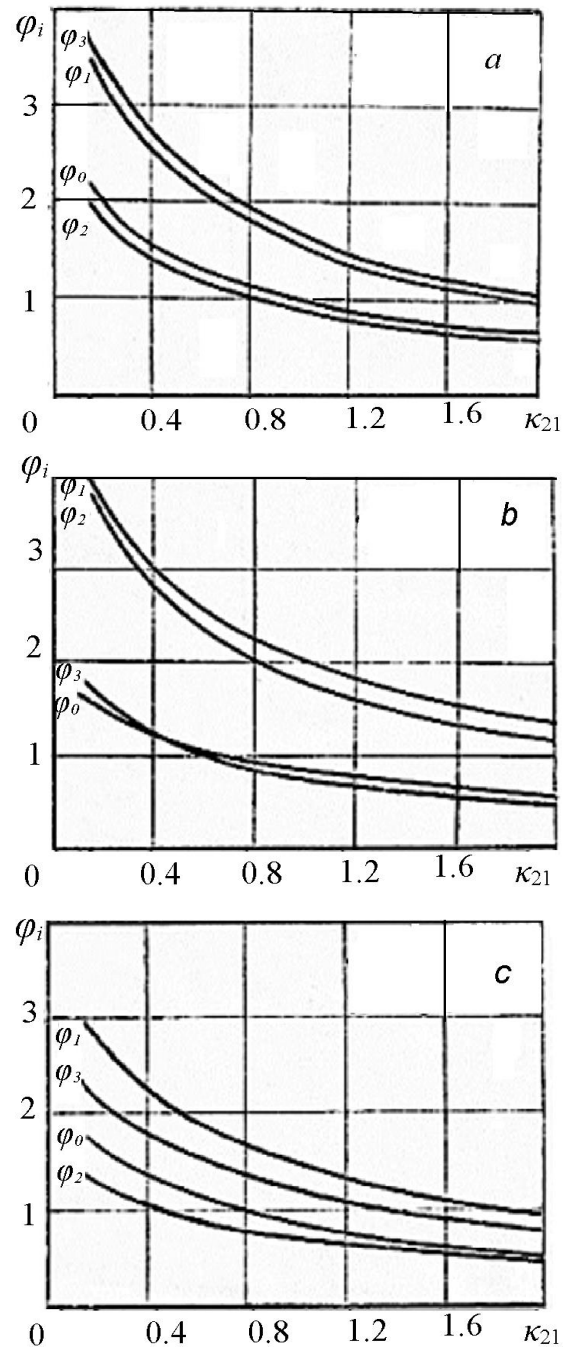


Fig. 1 Functions $A_i(i_0, \kappa_{21})$ versus κ_{21} for 3 values i_0 :
a) $i_0=0.3$, $\varphi_0=-A_0$, $\varphi_1=-10A_1$, $\varphi_2=-10^2A_2$, $\varphi_3=-10^4A_3$;
b) $i_0=1$, $\varphi_0=-10^2A_0$, $\varphi_1=-10^3A_1$, $\varphi_2=-10^4A_2$, $\varphi_3=-10^5A_3$;
c) $i_0=8$, $\varphi_0=-10A_0$, $\varphi_1=-10A_1$, $\varphi_2=-10A_2$, $\varphi_3=-10^2A_3$.

With a strong mixing in the injected phase, an initial part of a jet is comparably short independent on density ratio of the phases in a wide range tested from $i_0=0.3$ till $i_0=8$.

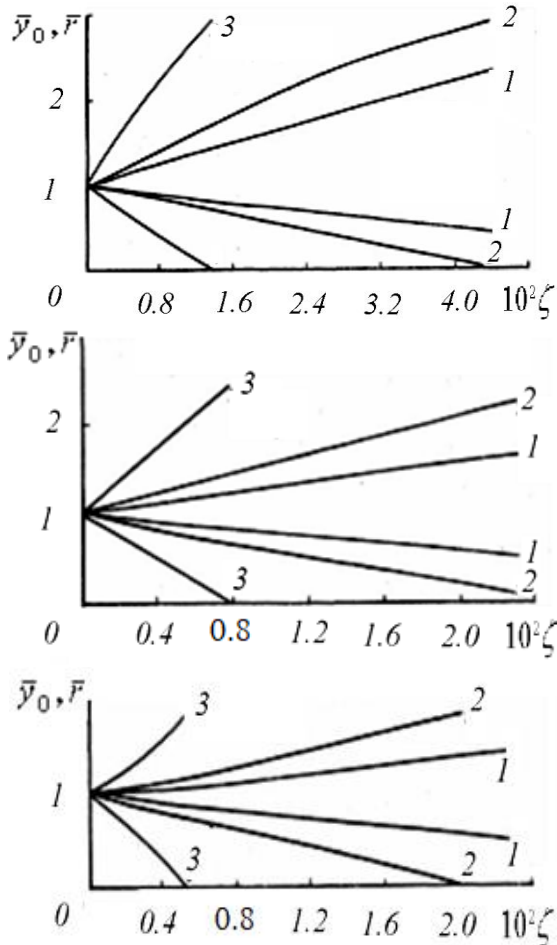


Fig. 2 Radiuses of jet's potential core \bar{y}_0 and mixing zone \bar{F} for the $i_0=0.3$, $i_0=1.0$, and $i_0=8.0$ from the top to the bottom picture, respectively:
1- $\kappa_{21}=0.2$, 2- $\kappa_{21}=1$, 3- $\kappa_{21}=5.0$

If the mixing coefficients in the phases are of the same order or coefficient in the ejected liquid is less than the one in a liquid going from the nozzle, the initial part of the jet is long (up to 5-10 times bigger than the radius of the jet nozzle). And the denser is the first liquid, the longer is an initial part of a jet.

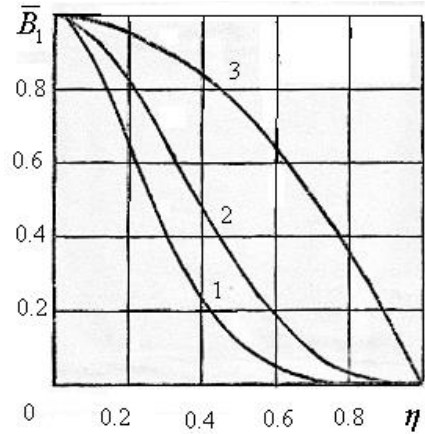


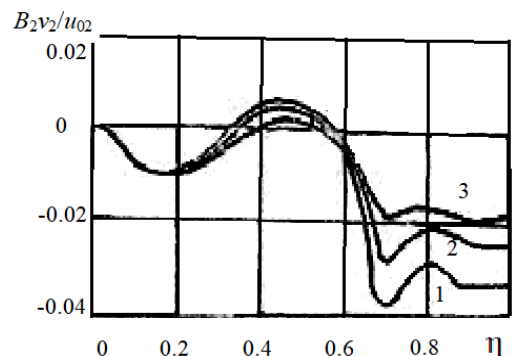
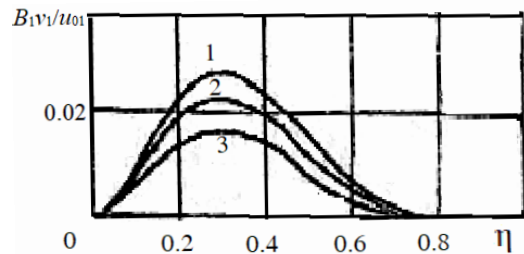
Fig. 3 Function-indicator for first phase across mixing layer: 1- $i_0=0.3$, 2- $i_0=1.0$, 3- $i_0=8.0$

The other characteristics of the initial part of a jet are presented in Figs 4-8. Here the turbulent shear in a jet, velocities by the phases, total velocity of the two-phase mixture and kinetic energy of the two-phase mixture are presented, correspondingly (x_i – the length of the initial part of a jet):

$$\bar{\tau} = \frac{\tau}{2\rho_1\kappa_1 u_{01}^2} = 6\eta(\eta-1)[\eta B_1 + i_0\kappa_{21}(1-\eta)B_2], \quad \frac{B_1 v_i}{u_{0i}}$$

$$\frac{v}{u_{01}} = \frac{B_1 v_1}{u_{01}} + s_0 \frac{B_2 v_2}{u_{02}}$$

$$\langle \overline{\rho u^2} \rangle = \frac{\langle \rho u^2 \rangle}{\rho_1 u_{01}^2} = B_1 \bar{u}_1^2 + i_0 B_2 \bar{u}_2^2.$$



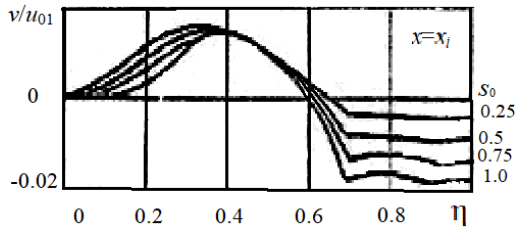


Fig. 4 Velocities of the phases v_1, v_2 and mixture of them v in 3 cross-sections by x (1- $0.33x_i$, 2- $0.67x_i$ and 3- $x=x_i$) for $i_0=0.3, \kappa_{21}=1, \kappa_1=0.006$

The profiles $B_1, B_1\bar{u}_1, \langle \rho u^2 \rangle = \frac{\rho u^2}{\rho_1 u_{01}^2}$ become

brighter, while the profile of an ejected phase $B_2\bar{u}_2$ is exhausting. The transversal velocity of the first phase is mostly directed to the external boundary of the mixing layer, while the second phase is moving in the opposite direction, to the axis of a jet. The tendency is clear by big values of the parameters i_0 , which is determined by the density ratio and by slip of the phases in a mixing layer.

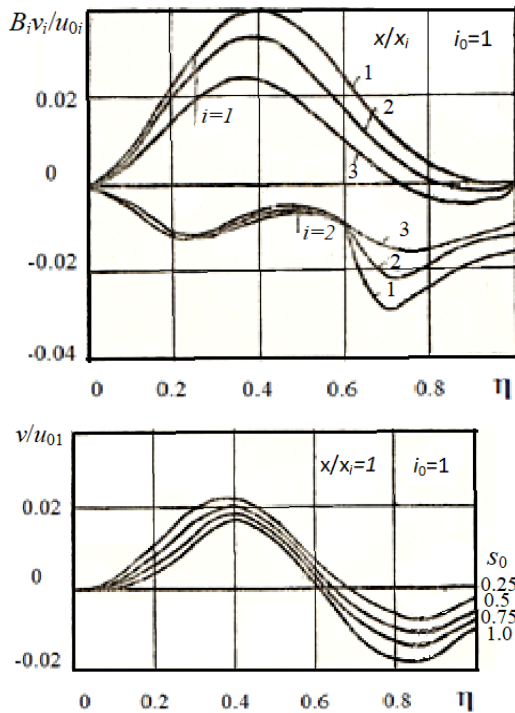


Fig. 5 Velocities of the phases v_1, v_2 and mixture of them v in 3 cross-sections by x (1- $0.33x_i$, 2- $0.67x_i$ and 3- $x=x_i$) for $i_0=1.0, \kappa_{21}=1, \kappa_1=0.006$

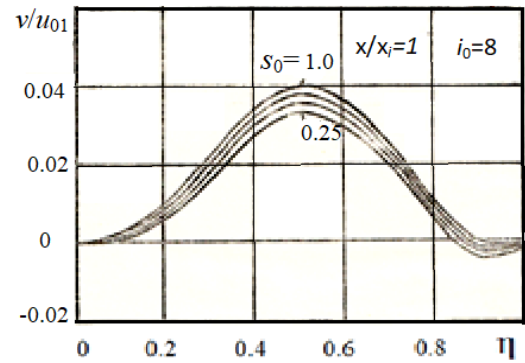
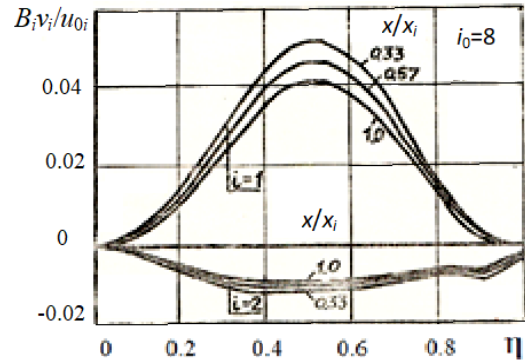
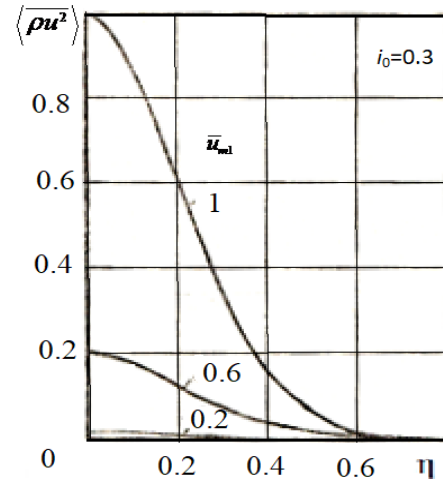


Fig. 6 Velocities of the phases v_1, v_2 and velocity of mixture v in 3 cross-sections by x (1- $0.33x_i$, 2- $0.67x_i$ and 3- $x=x_i$) for $i_0=8.0, \kappa_{21}=1, \kappa_1=0.006$



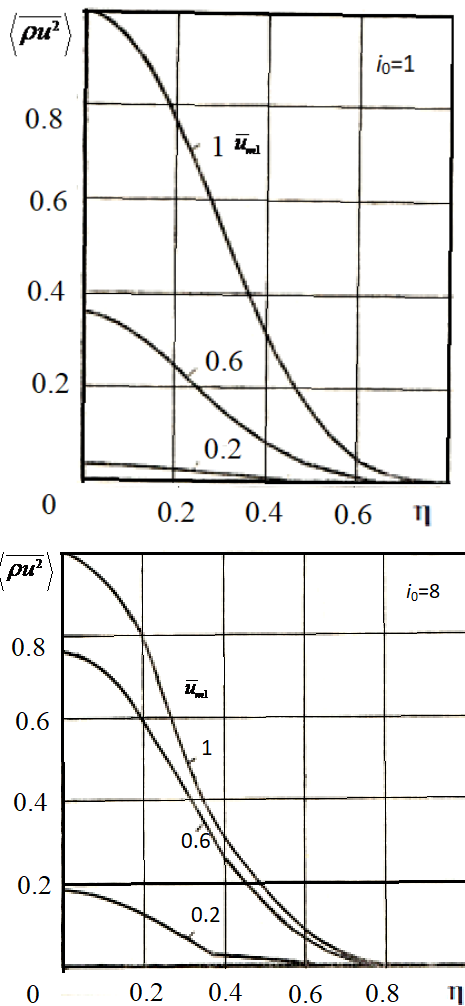


Fig. 7 Turbulent pulsation of energy across a layer, for: $\kappa_{21}=1$, $\bar{u}_{m1}=0.2, 0.6, 1.0$

2.2 Peculiarities of Jet Flow at Initial Part

The following peculiarities were revealed on the initial part of a jet. Increase of density leads to a shortening the length of an initial part. The profiles are close to the auto model ones. The maximal value of a turbulent stress in a flow with increase of the density of ejected liquid is shifted to the external boundary of the mixing layer.

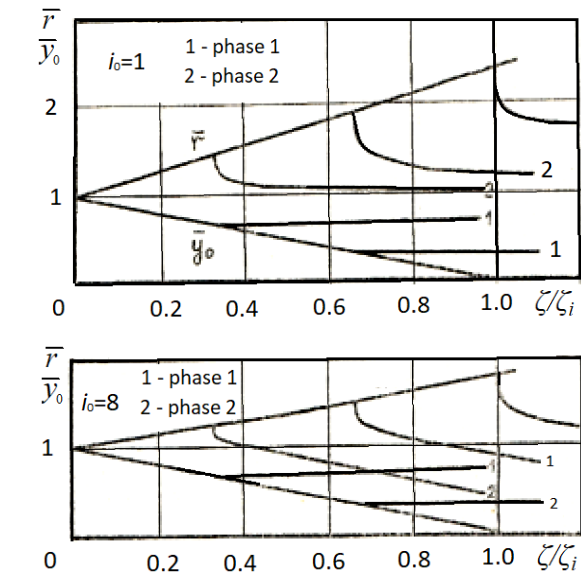
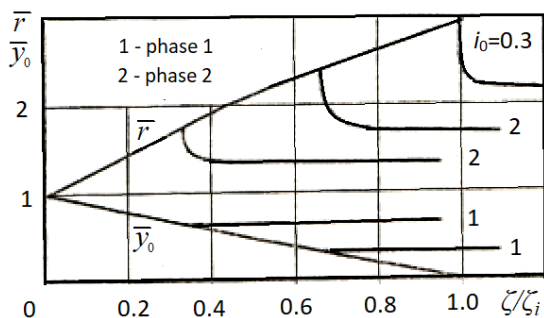


Fig. 8 Stream lines on initial part of two-phase jet: $\kappa_{21}=1$, $\kappa_1=0.006$

The trajectories of the phases in a mixing layer computed by the numerical solution of the boundary problem (1)-(3) are shown in Fig. 8. The first liquid tends to flow parallel to jet's axis by all density ratio, while the second phase is ejected into mixing layer more intensively with increase of density.

Remarkably the mixing of phases in a layer is very little and similar to all small density ratios up to 1 and even a little higher. Only by substantially denser second phase mixing is really intensive in the whole layer and the layer is comparably narrow. The real intensive mixing is seen by a high density ratio ($i_0 = ns_0^2=8$) but as far as this parameter i_0 contains the substantial influence of a slip of phases $s_0 = u_{02} / u_{01}$, which is falling down with an increase of the density ratio, then $i_0=8$ may correspond to a density ratio even higher than 8.

The stream lines are presented in Fig. 8 in relation to the length of the initial part (ζ/ζ_i), therefore a shortening of the initial part of a jet with increase of density of the ejected liquid was already accounted.

2.3 Estimation of the Transit Part of a Jet

The initial and the ground parts of a jet must be connected as shown in Fig. 9 [4]:

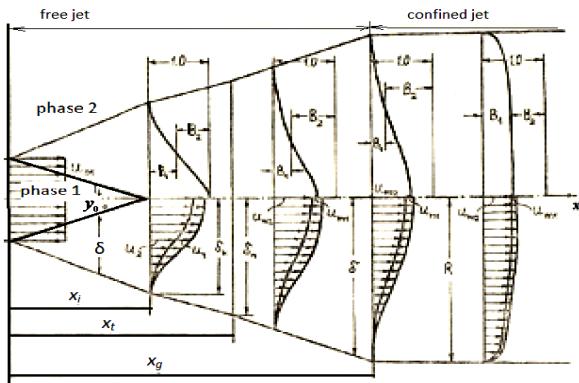


Fig. 9 Schematic representation of multiphase turbulent jet confined by channel at the distance x_g

For this, the length of a transient part of a jet was determined by interpolation of the external boundary of a jet from the initial to the ground part. This approximation was: $\delta = 1 + \alpha_1 \zeta + \alpha_2 \zeta^2$, where from the value x_r was computed by the known κ_1, δ_i . The value κ_1 was taken equal to the corresponding value at the initial part. The coefficients are:

$$i_0=0.3, \alpha_1=56, \alpha_2=-290; i_0=1.0, \alpha_1=57.5, \alpha_2=-250; i_0=8.0, \alpha_1=29, \alpha_2=600.$$

An interesting feature was revealed by the influence of parameters i_0, κ_{21} on a solution. The radius of a jet and velocities of phases (on the axis practically) do not depend on κ_{21} being totally determined by the value i_0 , while the functions B_{m1} and h strictly depend on κ_{21} . Thus, the turbulent mixing influences mostly the internal structure of a flow, while the distribution of phases and velocities depend on the density ratio of the phases (internal structure has a little influence on it).

Velocity distribution, in turn, determines a radius of mixing zone because it changes with falling of the velocity according to the mass and momentum conservation equations. With increase of κ_{21} , expansion of the jet intensifies. The turbulent stress is maximal approximately at the distance of about 1/3 of the mixing layer.

The transversal velocity of the first phase (ejecting liquid) B_{1v_1} is substantially lower than the one of the second phase (ejected liquid) B_{2v_2} , which is determining the transversal flow in a mixing layer. Independent of the value i_0 the velocity of the second phase is directed to an axis achieving the maximum on a distance about 0.5δ , decreasing with the growth of density of the ejected liquid.

2.4 Calculation of Jet Flow at Ground Part

The equation array (6), (8) with the boundary conditions (7) was solved as follows. From the (8) and the first equation (6), the u_{m1}, B_{m1} and $\delta=\delta_1$ were obtained as functions of the longitudinal coordinate ζ and parameters i_0, κ_{21} . The other radius of the turbulent zone $\delta=\delta_2$ was obtained from the second equation (6) by $\eta=\eta^*=0.5$. The computed velocity, function-indicator and the radius of turbulent mixing zone are given in Figs 10, 11:

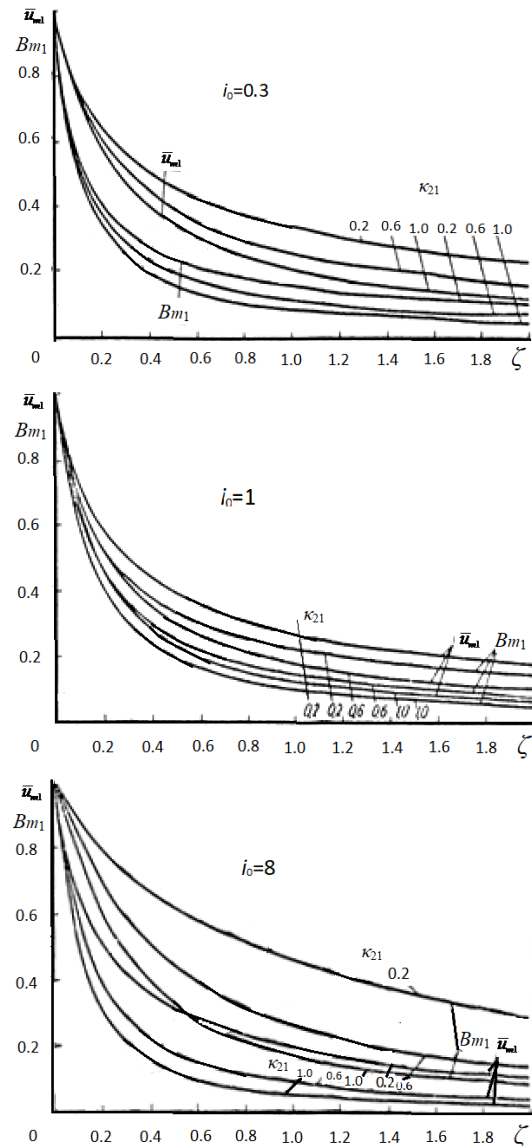


Fig. 10 Axial velocity and function-indicator for the jet along the axis: $i_0=0.3, 1, 8; \kappa_{21}=0.2, 0.6, 1.0$

In the next calculations, the value $\delta=\delta_1$ was accepted as a radius of a jet. Some of the computer simulations and the FORTRAN programs by the methodology described here first done by us were presented in [4, 5, 7]. Then it was further developed by Prof. Nakorchevskii with his co-workers, as well as by other researchers, e.g. [1, 6, 8, 9].

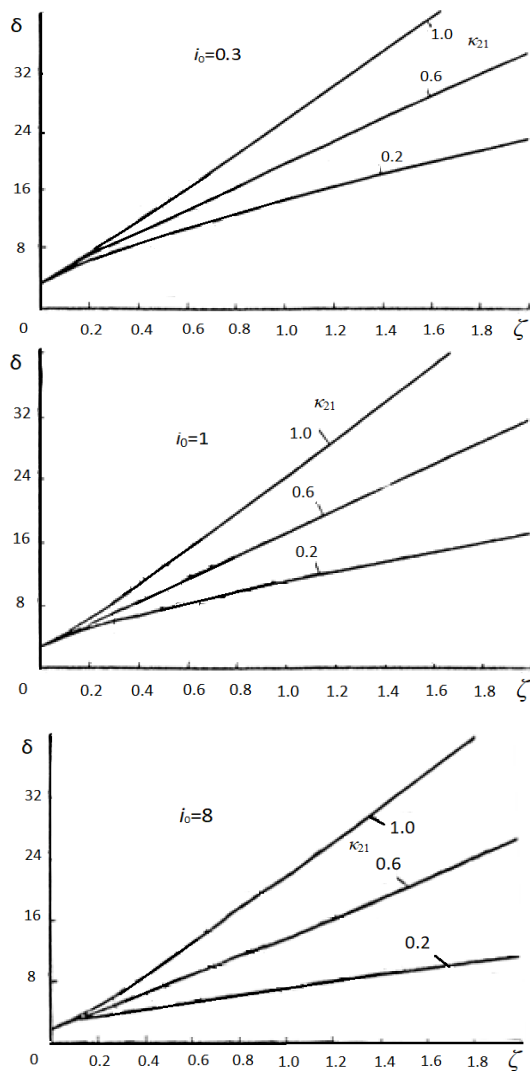


Fig. 11 Radius of the jet against the axial coordinate: $i_0=0.3, 1, 8$; $\kappa_{21}=0.2, 0.6, 1.0$

2.5 Validation of the Model Calculations against Experimental Data

Parameters of the turbulent two-phase jet, both analytical and numerical solutions obtained, have been compared against experimental data for the oil-water immiscible liquids as seen from the Fig. 12.

The special two-phase micro sensor was developed by Dr. V. Tinyakov from NTUU “KPI” for the experimental study of water jet in a pool with oil [4]. It measured parameters of the flow together with their belonging to a phase (function-indicator). Computational experiments revealed the basic features of the flow.

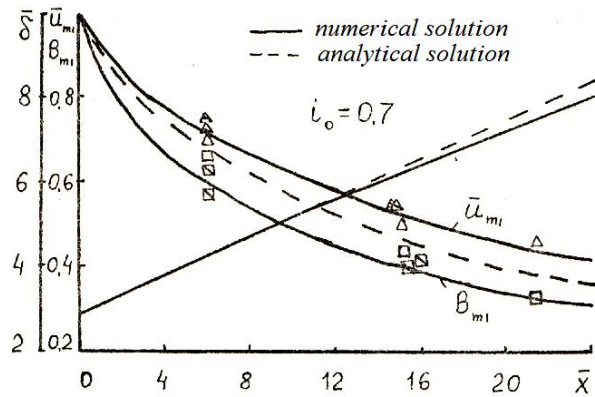


Fig. 12 Parameters of the turbulent two-phase jet against experimental data for oil-water: $i_0=0.7$

The results obtained have been compared to the experimental data of a number of researchers [4, 8-14]. The correspondence was good for the constants as follows: $i_0=0.3, \kappa_{21}=0.6$; $i_0=1, \kappa_{21}=0.4$; $i_0=8.0, \kappa_{21}=0.2$. Comparison with experimental data for the $i_0=0.7$ (oil-water) [4] obtained with using the two-phase sensor was the best at $\kappa_{21}=0.46$. Because the functions $\delta(\zeta, i_0)$ are close to the linear ones, an approximation $\delta(\zeta, i_0)=c_1+c_2\zeta$ was used. For $\kappa_{21}=0.5$, the first equation of the system (6) is simplified and solved analytically:

$$du_{m1} / d\zeta = -12u_{m1} / (c_1 + c_2\zeta),$$

which is the more precise, the closer κ_{21} is to 0.5. From the above-considered, it corresponds to $i_0 < 1$. The solution, with account of (8) and $\zeta = \infty$, $u_{m1}\delta = const$, $u_{m1}\delta^2 = \infty$, is as follows

$$u_{m1} = \delta_i / (\delta_i + 12\zeta), \quad \delta = \delta_i + 12\zeta. \quad (11)$$

The obtained results can be used in engineering computations and estimations, e.g. the correlation (11) for the radius of the mixing layer and velocity at the axis, as well as function-indicator of phases.

III. PHENOMENON OF THE JET ENERGY AMPLIFICATION FROM INPUT OF THE SURROUNDING LIQUID

This exciting phenomenon was first revealed by us at the end of 1970th [4, 5] for the high density of the surrounding liquid, by $i_0 \gg 1$, e.g. $i_0=8.0$, as shown for two-phase jet kinetic energy $\overline{\rho u^2}(\eta)$ and shear $\bar{\tau}$ for 3 values $i_0=0.3; 1.0; 8.0$ in Fig. 13. Parameter κ_{21} was varied from 0 to 1.

The phenomenon of amplification of a jet’s kinetic energy against the input energy of the first phase at its exit from the nozzle we could not prove experimentally due to serious impediments in

measuring. Despite the comparably small size of the two-phase sensor it was of the same order by size of the nozzle. Therefore, to locate sensor close to the nozzle was meaning to destroy the flow regime, while in the developed flow mixing layer it was much smaller comparing to the mixing layer radius.

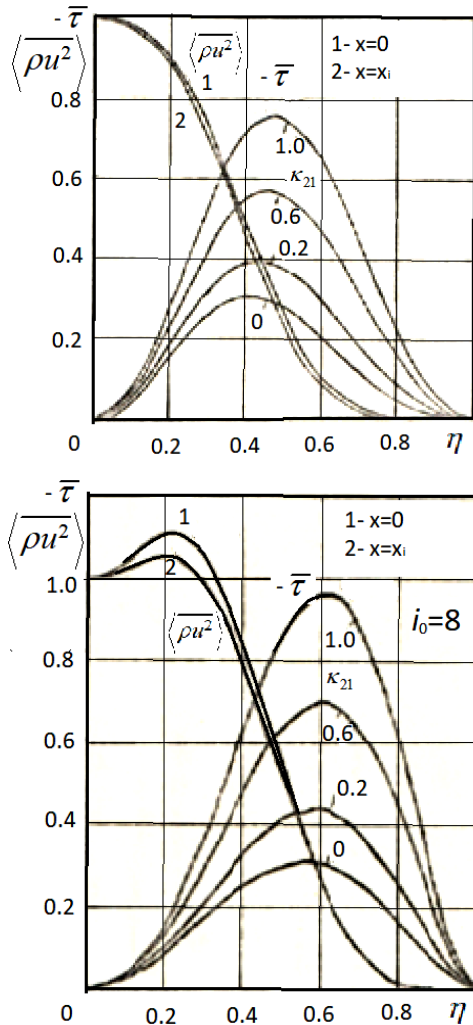


Fig. 13 Functions $\langle \rho u^2 \rangle(\eta)$ for $i_0=1.0$ and $i_0=8.0$

Moreover, in general the attainable accuracy of the turbulent mixing experiments was about 5-10%. Thus, it was close to the usual range of inaccuracy in turbulent flow experiments [14, 15]. Therefore, we have just carefully proved it theoretically. Later on, we have met a few reports in a literature mentioning the similar phenomena, mainly from the gas flows in the rocket engines [16, 17].

The causes of this effect and the source of additional energy were considered in [16] on a number of available mechanisms, e.g. acceleration of a jet caused not only by the inlet pressure, but also by the decrease in the potential energy of the current medium by reducing its absolute pressure down to the level of the technical vacuum.

Analysis of the above leads to conclusion that the effect studied by Kotousov can not only explain the mechanism of the operation of various hydrodynamic constructions (Schauberger, Clem, Cheryu, etc.) but also has tremendous practical value itself. Evidently the simple models of the turbulent jets like the one used here are far from reality in some aspects, though they are in good correspondence with the experimental data.

IV. MODELING OF HEAT-MASS TRANSFER IN THE MELT JETS WITH VOLATILE COOLANT

The method was applied to a modeling of the complex two-phase flows for the corium cooling during severe accidents at NPP [9, 18] and for the new jet type machines for steel melting [19].

The two-phase turbulent flow of melt with vapor is shown in Fig. 14. For $i_0 > 3$, h is in the range from 0 to -6. By $i_0 \gg 3$, h was computed for the initial part of jet:

$$h_0 = \frac{0.0054i_0 - 0.0860}{0.0069 + 0.0048i_0}, \quad h_i = \frac{0.0023i_0 - 0.0469}{0.0016i_0 + 0.0042}$$

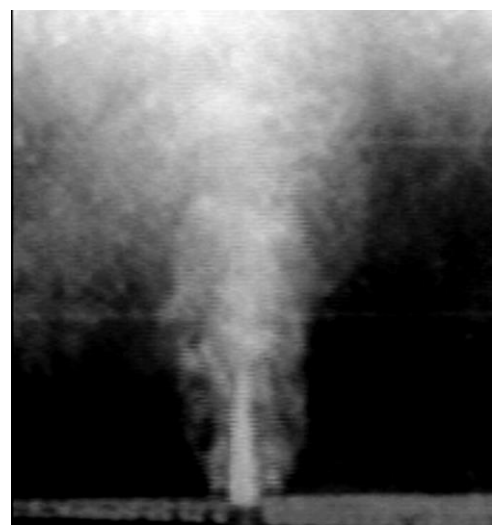


Fig. 14 Jet of volatile coolant penetrating the pool of melt from below [9]

Because the maximal value for h is 0 (B_1 cannot exceed 1), it yields: $h_0=0$, then $\max i_0=16$ approximately. By this value i_0 , the slip of phases is estimated as $s_0 = 4\sqrt{\rho_{12}}$, so that if $\rho_{21} = 400$, then $u_{02}=2u_{01}$ for the initial part of a jet. In a similar way, $h_i=0$, $\max i_0=20.4$ and $s_0 = 4.52\sqrt{\rho_{12}}$ for the end of the initial part of the jet, so that the difference s_0 at the initial part of jet is about 13% total.

The constants were as follows

$$\begin{pmatrix} a_{11} & a_{12} & b_{11} & b_{12} \\ a_{21} & a_{22} & b_{21} & b_{22} \\ a_{31} & a_{32} & b_{31} & b_{32} \\ a_{41} & a_{42} & b_{41} & b_{42} \end{pmatrix} = \begin{pmatrix} 0.5464 & 0.0208 & 0.0179 & -0.0101 \\ 0.1667 & 0.0101 & 0.0095 & -0.0042 \\ 0.4604 & 0.0139 & 0.0054 & -0.0048 \\ 0.1198 & 0.0059 & 0.0023 & -0.0016 \end{pmatrix}$$

The volumetric ejection coefficient and the expansion rate for the end of the initial part of a jet are the following: $q_1=0.013$, $\delta_1=1.73$. As it was shown, the entrainment is very small and the expansion is less than 2.

For the beginning of ground part of the jet from (15) yields:

$$\begin{pmatrix} \alpha_{11} & \alpha_{12} & \beta_{11} & \beta_{12} \\ \alpha_{21} & \alpha_{22} & \beta_{21} & \beta_{22} \end{pmatrix} = \begin{pmatrix} 0.1286 & 0.0071 & -0.0905 & -0.0040 \\ 0.0792 & 0.0033 & -0.0501 & -0.0016 \end{pmatrix}$$

$\beta_{10} = 0.1$, $\beta_{20} = 0.052$, and then

$$h_i = \frac{0.0023i - 0.0494}{0.0016i + 0.0038}, \quad \delta_i = \frac{1}{\sqrt{2(0.0071h_i + 0.1286)}}$$

The maximal $h_i=0$, therefore $\max i=21.48$, $\max s = 4.64\sqrt{\rho_{12}}$, or by the above parameters $\max s=0.232$, $\delta_i=1.97$. The following boundary problem for the ground part is resulted:

$$B_{m1} = \frac{1.13\bar{u}_{m1}}{0.13 + \bar{u}_{m1}}, \quad \delta = \frac{1.97}{\bar{u}_{m1}} \sqrt{\frac{0.13 + \bar{u}_{m1}}{1.13}}$$

$$\frac{d\bar{u}_{m1}}{d\zeta} = -\frac{6.46\bar{u}_{m1}^2}{\sqrt{0.13 + \bar{u}_{m1}}} \frac{\bar{u}_{m1} + 5\kappa_{21}(1 - \bar{u}_{m1})}{2.5 - 1.5\bar{u}_{m1}}$$

It was solved numerically for $\kappa_{21} \in [0.1, 1.0]$.

Simulation of the cooling of melt pool with volatile coolant was done. The integral entrainment of the melt into a mixing layer of coolant was

$$Q = 1/H \int_0^H q(x)dx, \quad \text{and} \quad Q = 1/H \sum_{i=1}^N q(x_i)(x_i - x_{i-1}),$$

where H is the height of the pool, $q(x_i)$ is the ejection coefficient, x_i is a current point in a partition of the calculated interval by x . The time pass for vapor through the pool is

$$\Delta t = H / u, \quad u = 1/H \sum_{i=1}^N u_{mi}(x_i - x_{i-1}),$$

u is the mean velocity of vapor in a mixing layer.

Assuming that every portion of coolant vaporizes near the nozzle, a heat removal from melt by a coolant is got according to the heat balance:

$$c_2 M_2 (T_{20} - T_2) = q_c \Delta t h_{lv},$$

where q_c is the coolant's flow rate, h_{lv} is a heat of vaporization, T_{20} , T_2 are the initial and current temperatures of melt, respectively, M_2 is a mass of melt in a pool to be cooled.

The melt's temperature is

$$T_2 = T_{20} - q_c \Delta t h_{lv} / (c_2 M_2).$$

Then the heat balance for one portion of vapor going from the nozzle to a top of the pool is expressed: $c_2 \rho_2 Q V (T_2 - T) = c_1 \rho_1 (1 - Q) V (T - T_1)$, where V is the total volume of a mixing zone and T is the equilibrium temperature after heat exchange:

$$T = \frac{c_2 \rho_2 Q T_2 + c_1 \rho_1 (1 - Q) T_1}{c_2 \rho_2 Q + c_1 \rho_1 (1 - Q)}$$

Assuming that vapor is going off the pool from a free surface and the drops are falling down into a pool, an account of the melt's cooling with such drops is: $m_t T + (M_2 - m_t) T_2 = M_2 T_2$, where m_t is the mass of the drops in a jet, which is as follows:

$$m_t = 0.25\pi Q \rho_2 (\bar{\delta} + 1)^2 H r_0^2.$$

Afterward, the correlated temperature of a melt due to one cycle of a jet passage through the melt pool is got. Step-by-step, the temperature of a melt with time was computed: $n=0.27$, $\kappa_{21}=0.6$; $n=1.0$, $\kappa_{21}=0.4$; $n=7.3$, $\kappa_{21}=0.2$. The following approximation satisfied these data:

$$\kappa_{21} = 0.4 - 0.1326 \ln n + 0.0163 (\ln n)^2,$$

where from the minimal value of κ_{21} is 0.13. For the big values of n it was stated $\kappa_{21}=0.1$ in this case.

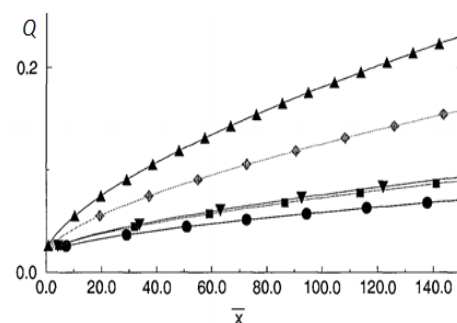
The thermal parameters governing the boiling process were studied in [18]. First, the averaged values κ_1 were got from the experiments (Table 3):

Table 3. Experimental data [9]: $r_0=0.3$ mm,

$$\mu_1 = 2 \cdot 10^{-5} N \cdot s / m^2, \quad \rho_1 = 2.1 \text{ kg} / m^3$$

Cases	κ_1		$u_{0,i}$ (m/sec)		$\rho_{2,1}$		$\mu_{2,1}$ (20°C)	
	water	paraf.	water	paraf.	water	paraf.	water	paraf.
(a)	0.008	0.016	0.23	0.29	476	419	4.16	271
(b)	0.031	0.007	0.29	0.59	476	419	4.16	271
(c)	0.058	0.014	0.59	0.17	476	419	4.16	271
(d)	0.014	0.009	0.29	0.29	476	419	4.16	271
(e)	0.008	0.014	0.59	0.47	476	419	4.16	271
(f)	0.012	0.011	0.29	0.59	476	419	4.16	271
(g)	0.012	0.011	0.59	0.77	476	419	4.16	271
(h)	-	0.012	-	1.01	-	419	-	271

Then the characteristic parameters were computed and presented in Figs 15-17:



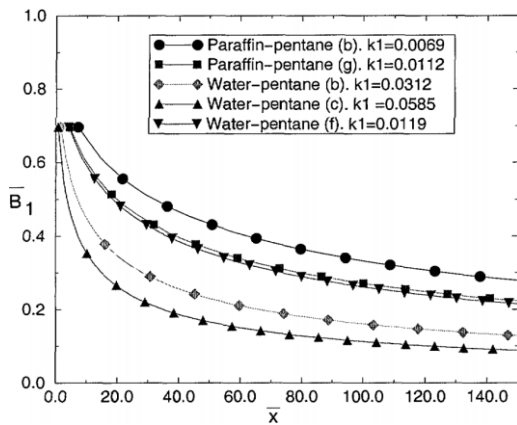


Fig. 15 Tendency of flow rate Q and function-indicator B_1 for different flow cases [9]

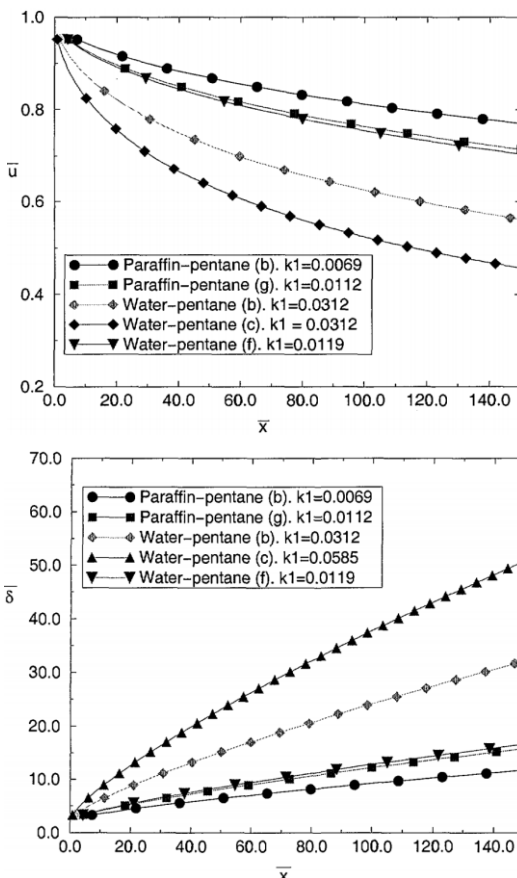


Fig. 16 The flow velocity and width of the mixing zone for flow different cases [9]

As seen from the results in Figs 15-17, the method is good for such complex two-phase jets. It allows computing the important two-phase characteristics for the estimation of cooling processes with the liquid metal corium and volatile coolant. The problem is of paramount importance for the modeling and simulation of the severe accidents at the nuclear power plants. By the results of such modeling it is available to choose the right parameters of the passive protection systems against the severe accidents.

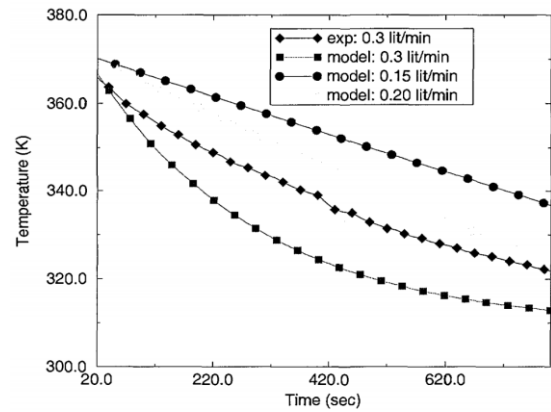


Fig. 17 Comparing the temperature profile for the model and experiment [9]

Despite in this case the density ratio is much bigger in the above considered case of mutually immiscible liquids, the correspondence of the calculating and experimental data is achieved reasonable. Here it is extremely important to have calculation of the parameters in two-phase mixture because it allows computing heat transfer from one phase to another one, which is determined by the spatial phase distribution. Thus, the method has been proven for diverse physical situations successful.

The next paper is devoted to application of the method to the numerical simulation of the heterogeneous turbulent jet of two mutually immiscible liquids, which is confined by cylindrical channel on some distance from the nozzle.

V. CONCLUSION

The turbulent mixing in jet flows of mutually immiscible liquids is complex process. This attempt is interesting both, in theoretical and practical aspects because revealed some features of the two-phase flow. The presented method of mathematical modeling and computer simulation is accounting the distribution of the phases in mixing layer of two immiscible liquids that is highly important for deep understanding and optimization of the diverse mixing processes including the turbulent two-phase jet flows.

The method proposed by Prof. Nakorchevskii has been successfully realized. It is easy to implement into calculation of the parameters for many other turbulent multiphase flows. Comparison of the calculations by presented method has been successfully done during the years for the turbulent jets of the oil and water using the specially constructed two-phase sensors. Later on, it was computed and compared against experimental data

for the modeling of the corium melt cooling with the volatile coolant.

The method with using the function-indicator for the spatial phase distribution in the turbulent jet flows is original and has advantage in possibility for investigation of the real two-phase flow mixtures. Using the function-indicator, it is available to connect the calculated characteristics of the two-phase flow with the experimental data by distribution of the phases in mixing, which is very important for the multiphase flows.

The disadvantage of the method is application of the polynomial approximations for the velocities of the phases and for the function-indicator, which are not developed so well for some flows different from the jet flows. Also there is the piece-wise approximation of the function-indicator, therefore it is needed to control the required approximation during the calculation process and change it according to the range of validity of approximation.

References:

- [1] Kazachkov Ivan V. Mathematical Modeling of the Mixing and Heat Transfer in Turbulent Two-Phase Jets of Mutually Immiscible Liquids// WSEAS Transactions on Heat and Mass Transfer, 2020, 15 (16), p. 117-129.
- [2] Samarinas N., Tzimopoulos C. and Evangelides C. Fuzzy Numerical Solution to Horizontal Infiltration// International Journal of Circuits, Systems and Signal Processing, 2018, Vol. 12, p. 325-332.
- [3] Cannata G., Gallerano F., Palleschi F., Petrelli C., and Barsi L. Three-dimensional numerical simulation of the velocity fields induced by submerged breakwaters// International Journal of Mechanics, 2019, Vol. 13, p. 1-14.
- [4] Nakorchevskii A.I. Heterogeneous turbulent jets: the theory and experimental investigation. Kyiv: Naukova Dumka, 1980, 142 pp.
- [5] Nakorchevskii A.I., Kazachkov I.V. Calculation of heterogeneous turbulent jet. In book: Automation Systems of continuous technological processes, Institute of Cybernetics of NASU, 1979, p. 68-79.
- [6] Kazachkov I.V. Approaches for mathematical modeling and experimental study of the turbulent flows of mutually immiscible liquids (oil-water)// International Journal of Petroleum and Petrochemical Engineering (IJPPE), 2018, 4(1), p. 70-81.
- [7] Kazachkov I.V., Nakorchevskii A.I. The stream lines in a turbulent two-phase jet of two immiscible liquids/ Abstracts of the V All SU Meeting on Theoretical and Applied Mechanics. Alma-Ata, 1981 (In Russian).
- [8] Nakorchevskii A.I., Basok B.I. Hydrodynamics and heat transfer in heterogeneous systems and devices of pulsating type. Kyiv: Naukova Dumka, 2001, 348 pp.
- [9] Kazachkov I.V., Paladino D. and Sehgal B.R. Ex-vessel coolability of a molten pool by coolant injection from submerged nozzles/ 9th International Conference on Nuclear Energy Development. April 8-12, 2001. Nice, France.
- [10] Nakoryakov V.E., Pokusaev B.G., Shreiber I.R. Spreading of the waves in gas- and vapor-liquid media. Novosibirsk: Institute of Thermal Physics, 1983, 238 pp. (In Russian).
- [11] Nigmatulin R.I. and Friedly J.C. Dynamics of Multiphase Media. CRC Press: Volumes 1 & 2. Revised and Augmented Edition (v. 1 & v. 2), Oct 1, 1990, 878 pp.
- [12] Ginevskii A.S. The theory of turbulent jets and traces. Integral calculation methods. Moscow: Mashinostroenie, 1969, 400 p. (In Russian).
- [13] Kolev N.I., Multiphase Flow Dynamics 1. 2015. Springer International Publishing. 840 pp. (totally 5 volumes by different applications including thermo hydraulics in nuclear energy processes).
- [14] Abramovich G.N. (Volume editor Leon Schindel). Theory of Turbulent Jets Cambridge, Mass., USA: MIT Press.- 1963, 671 pp.
- [15] Yakovlevskiy O.V. The Mixing of Jets in a Channel with Variable Cross Section// Izvestiya Akademii NaukSSSR, OTN, Mekhanika i Mashinostroyeniye, 1962, No. 1, P. 66-72 (English translation FTD-TT-62- 1571).
- [16] Kotousov L.S. Measurement of the Water Jet Velocity at the Outlet of Nozzles with Different Profiles// Technical Physics, 2005, 50 (9), p. 1112–1118.
- [17] USSR invention No.314 year 1986 Register “Phenomenon of abnormal high thrust increase in gas ejection process with pulse active jet”.
- [18] Paladino D. Investigation of mechanisms for melt coolability with bottom coolant injection. Licentiate Engineering Thesis, Royal Institute of Technology (RIT/NPS), 2000.
- [19] Nakorchevskii A.I. Reactor for continuous refinement of metal/ Patent USSR №492554. Bulletin, 1975, №43.